



INTERNATIONAL ATOMIC ENERGY AGENCY  
UNITED NATIONS EDUCATIONAL, SCIENTIFIC AND CULTURAL ORGANIZATION  
**INTERNATIONAL CENTRE FOR THEORETICAL PHYSICS**  
I.C.T.P., P.O. BOX 586, 34100 TRIESTE, ITALY, CABLE: CENTRATOM TRIESTE



UNITED NATIONS INDUSTRIAL DEVELOPMENT ORGANIZATION



**INTERNATIONAL CENTRE FOR SCIENCE AND HIGH TECHNOLOGY**

174 INTERNATIONAL CENTRE FOR THEORETICAL PHYSICS 34100 TRIESTE (ITALY) VIA GARGANO, 9 (ADRIATICO PALACE) P.O. BOX 586 TELEPHONE 040/22472 TELEFAX 040/22473 TELEX 40049 APN I

SMR/760-34

**"College on Atmospheric Boundary Layer  
and Air Pollution Modelling"  
16 May - 3 June 1994**

---

"Wind-Field and Dispersion-Modelling in Built-Up Areas"

R. ROECKLE  
Tüv Energie und Umwelt GmbH  
Freiburg, Germany

***Please note: These notes are intended for internal distribution only.***

## Wind field- and dispersion-modelling in built-up areas

Dr. Rainer Röckle

TÜV Energie und Umwelt GmbH  
Robert-Bunsen-Straße 1,  
D-79108 Freiburg  
Germany

### Abstract

This lecture presents some modules to calculate wind fields and immissions in the nearfield of buildings. Results of a running research project are shown, where numerical simulation results of several models are compared to systematic wind tunnel studies. Further some examples of characteristic projects will show the efficiency of the diagnostic model ABC.

### Introduction

In a engineering office like the TÜV we are often confronted with questions to climatic and air pollution changes by planned buildings or building clusters. Some typical topics are:

- Dispersion of traffic exhaust gases
- Dispersion of toxic gases caused by accidental releases in industrial plants
- Ventilation changes in cities caused by blocking structures
- Determination of locations with speed-up zones (wind-comfort)

In the planning stage different conceptive alternates can be regarded. To quantify the effects under the limitations in costs and time, efficient numerical models have to be used. The complexity of structures in built-up zones implies the use of 3-dimensional models.

The models described here are composed of the modules:

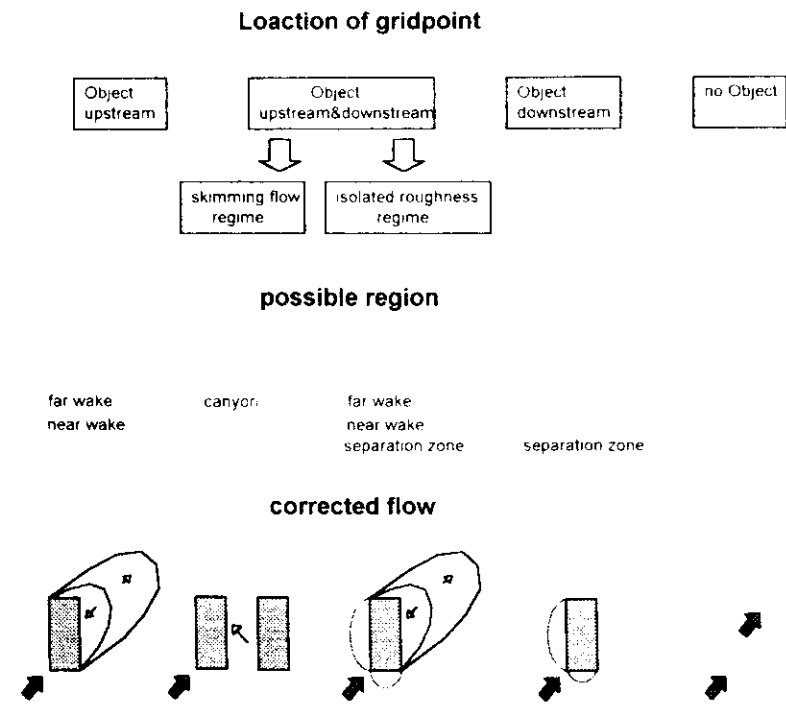
- mean wind field calculation
- evaluation of turbulence parameters
- and finally the dispersion module.

Another module for grid based dispersion models is the emission model. In case of line-, area- or volume-sources the calculation of an emission inventory is necessary.

### 2. Simulation of flow fields

An effective way to compute flow fields is a diagnostic scheme. Physically the conservation of mass is guaranteed. All other physical characteristics of the flow, for example the development of recirculation zones, have to be considered in the initialisation procedure. The model **DASIM** ("DArmstädter Simulations Modell", Blinda et al. 1992) and the model **ABC** ("Airflow around Building-Clusters", Röckle 1990) are two similar diagnostic microscale models, which produce mass-consistent, three-dimensional mean wind-fields, using such an "intelligent" initialisation procedure.

The initial wind field was furnished by an objective procedure, which analyses the building structure at each grid point. In ABC four possibilities are distinguished according to the following sketch:



In a first step the wind components were set to the values of the approach flow. Then these components are modified according to the distance from the obstacles following measurements from wind tunnel (a summary is given in Hosker, 1984):

- reversed flow within the near wake
- decreased flow within the far wake
- no flow within the separation zones
- reversed component perpendicular to the canyon axes within canyon-type situations

This wind field is adjusted in a least-squares sense with variational-techniques to satisfy the continuity equation (Sasaki 1970, Sherman 1978)

The Poisson-equation to be solved for  $\lambda$  is given by

$$\frac{\partial^2 \lambda}{\partial x^2} + \frac{\partial^2 \lambda}{\partial y^2} + \left( \frac{\alpha_h}{\alpha_v} \right) \frac{\partial^2 \lambda}{\partial z^2} = -2\alpha_h \left( \frac{\partial u^0}{\partial x} + \frac{\partial v^0}{\partial y} + \frac{\partial w^0}{\partial z} \right) \quad (1)$$

where  $\lambda(x,y,z)$  is the lagrange multiplier,  $u^0$ ,  $v^0$  and  $w^0$  is the initial wind field and  $\alpha_h, \alpha_v$  are Gauss precision moduli. Different values of  $\alpha_h$  and  $\alpha_v$  allow to distinguish between the adjustments made to horizontal and vertical velocity components (large values imply minimal adjustments)

The final divergence free wind field ( $u, v, w$ ) is achieved by setting  $\lambda$  into the Euler-Lagrange equations

$$\begin{aligned} u &= u^0 - \frac{1}{2\alpha_h} \frac{\partial \lambda}{\partial x} \\ v &= v^0 - \frac{1}{2\alpha_h} \frac{\partial \lambda}{\partial y} \\ w &= w^0 - \frac{1}{2\alpha_v} \frac{\partial \lambda}{\partial z} \end{aligned} \quad (2)$$

Upper and lateral boundaries of the computational-area are regarded to be open - thus allowed mass flow through the boundaries. The bottom boundary and the walls of the structures are assumed to be solid - thus no mass can flow through these boundaries

The calculations are based on a cartesian coordinate system with a staggered grid (Fig. 1). The horizontal grid width varies typically from 1 to 10 m. The vertical grid is variable spaced with higher resolution ( $\Delta y \approx 1-3$  m) near to the ground

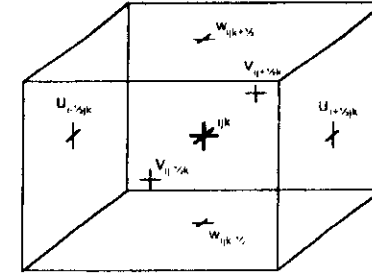


Figure 1: grid used in DASIM and ABC

The model calculates very detailed wind fields on a large number of grid points in a small amount of computer time (a 640kB PC-System solves  $40 \times 40 \times 12$  grid points in a few minutes)

The specific types of flow near obstacles can be found on model output (Fig. 13). These are recirculation areas, sheltered areas, speed-up zones, channelling within street canyons and vortex formation behind sharp edges

## 2. Turbulence parameters

The dispersion models used are solving the advection-diffusion equation of the form

$$\frac{\partial C}{\partial t} + u \frac{\partial C}{\partial x} + v \frac{\partial C}{\partial y} + w \frac{\partial C}{\partial z} + \frac{\partial}{\partial x} \left( K_x \frac{\partial C}{\partial x} \right) + \frac{\partial}{\partial y} \left( K_y \frac{\partial C}{\partial y} \right) + \frac{\partial}{\partial z} \left( K_z \frac{\partial C}{\partial z} \right) = P + S \quad (3)$$

where  $u$ ,  $v$  and  $w$  are the calculated wind components,  $K_x$ ,  $K_y$  and  $K_z$  are the turbulent diffusion coefficients in the  $x$ -,  $y$ - and  $z$ -directions,  $P$  is the production term and  $S$  sink terms (chemical removal, deposition). Shir and Bomstein (1977) stated an approach of the necessary diffusion coefficients for non-homogeneous terrain

$$K = l^2 S \quad (4)$$

where  $l$  is a mixing length, in ABC defined as the nearest distance to the closest surface (obstacle or ground), and the quantity  $S$  is related to the divergence and deformation of the flow field

$$S = \sqrt{2D_{xx}^2 + D_{yy}^2 + D_{zz}^2 + D_{xx}^2} \quad (4a)$$

with

$$D_0 = \left(\frac{du}{dx}\right)^2 + \left(\frac{dv}{dy}\right)^2 + \left(\frac{dw}{dz}\right)^2$$

$$D_{11} = \left(\frac{du}{dy} + \frac{dv}{dx}\right) ; \quad D_{12} = \left(\frac{du}{dz} + \frac{dw}{dx}\right) ; \quad D_{22} = \left(\frac{dv}{dz} + \frac{dw}{dy}\right)$$

ABC calculates K-values on the midpoint of the staggered grid and interpolates these values on the velocity grid, while DASIM calculates them in a direct manner on the velocity grid.

Another way to determine diffusivities is described by Groß et.al.(1994). In his model ASMUS ("Ausbreitungs- und StrömungsModell für Urbane Strukturen") he solves iteratively the equation for the turbulent kinetic energy E with the transport and diffusion terms, the dynamic production, the buoyancy term and the molecular dissipation:

$$0 = -u_i \frac{\partial E}{\partial x_i} + \frac{\partial}{\partial x_i} \left( K \frac{\partial E}{\partial x_i} \right) + K \left( \frac{\partial u_i}{\partial x_j} + \frac{\partial u_j}{\partial x_i} \right) \frac{\partial u_i}{\partial x_j} - K \frac{g}{\Theta} \frac{\partial \Theta}{\partial x_i} \delta_{ij} - \frac{E^{3/2}}{a \cdot l} \quad (5)$$

l is a characteristic length (for example  $l = (\Delta x \cdot \Delta y \cdot \Delta z)^{1/3}$ ), a an empirical constant (0.4), g the gravitational constant and  $\Theta$  the potential temperature. The diffusion coefficients can be calculated according the Prandtl-Kolmogorov equation

$$K = a l \sqrt{E} \quad (6)$$

The real problem in parameterization of the turbulence is the lack of measured data to verify these relations. This is even true for other dispersion models, where other closures are needed, for example particle models which use Lagrangian time scales.

### 3. Dispersion models

The mass-consistent, three-dimensional wind fields are necessary input for a pollutant transport model. The physical processes to be described by the pollutant model are advection, turbulent diffusion and if necessary removal by (linear) chemistry.

The advection-diffusion equation (3) is solved on an Eulerian grid, using a time split scheme. In order to determine the concentrations in the boxes, a mass-budget is computed from the difference of the inflow and outflow of material through the boundaries and the amount of sources (emissions) and sinks (chemical removal).

The time-step is variable and depends on wind-velocity, diffusion coefficients, grid size and decay-terms.

Both models ABC and DASIM use this scheme. The disadvantage of procedure is the relatively big amount of computer time to get stationary concentration fields, because the calculated time steps are very small (typical below 1 s). If only stationary concentrations are of interest, a faster method is given in ASMUS, which solves the stationary form of equation (3) with a SOR-technique.

### 4. Comparison to wind tunnel results

Together with the wind tunnel section of the University of Karlsruhe (Prof. Plate) we started a research project funded by the State of Baden-Württemberg and the Commission of the European Communities.

The aims of this project are

- to clear up deficiencies in models to enable corrections and further developments,
- the valuation of error-margins and
- the creation of a verification-base for other model-investigators

The selected obstacles are three U-shaped buildings and a small area in an industrial complex. In the comparison take place

- MISKAM, a prognostic model (Eichhorn 1989),
- ABC and DASIM
- ASMUS (turbulence and dispersion part, wind field from ABC)
- LASAT from Janicke (1985), lagrangian dispersion model (comparison is still in work)

To study the quality of the flow- and dispersion models in the nearfield of a "complex" body, a U-shaped structure was chosen (Fig. 2). The height of the structure varies from 16 m over 28 m to 40 m. The dimensions of the courtyard are 28 m · 28 m. The width of the buildings is 12 m. According to the approach flow, different vortex systems within the courtyard are expected.

Up to 6 wind directions are chosen, 0°, 45°, 90°, 120°, 135° and 180°. The power law profile of the approach flow was adjusted to an exponent of 0.28 and the wind speed at 10 m above ground to 5 m/s.

Three sources are regarded:

- Source A – 2 m above the roof level of the mid building
- Source B – 2 m above ground in the courtyard
- Source C – 2 m above ground in front of the building

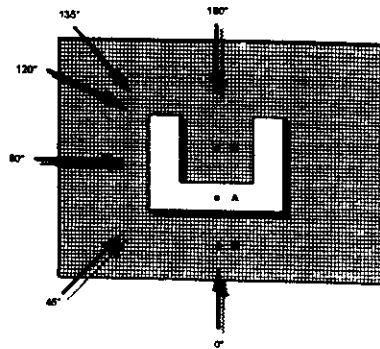


Figure 2. Wind directions and location of sources

The basic questions are

- Can the models simulate this in a satisfying manner?
- What is the range of the error margins?
- In which module does the errors occur?

In wind tunnel many horizontal and vertical profiles of concentrations were measured. The measurement of mean wind speed and direction is only for a few cases available

Measured and calculated concentrations are compared at distinct points. One should keep in mind, that the measurements are point values and the calculated concentrations represent volume averaged values

#### 4. Results

Figure 3 shows some differences in the near ground flow field between the models ABC and MISKAM. MISKAM simulates a relatively short recirculation zone, but gives better results near the upwind edges of the building.

In Figure 4 there are four vertical sections at the centre of the U-shaped building with an approach flow normal to the U. Differences in the near wake field and in the front of the buildings can be detected. The last picture shows wind tunnel measurements. DASIM shows the best results on the roof and within the courtyard. The separation of the flow takes place at the upwind edge of the roof and don't reattach to it. However the longitudinal extend of the wake is not realistic.

On Figure 5 the diffusion coefficients are displayed. The lines of constant K-values (mean values on staggered grids) are numbered in  $m^2/s$ . Big variances between the models can be found. The mixing length

concept of some schemes are not satisfying. The best results were produced by the more sophisticated ASMUS method.

The next figure (6) gives an impression how transport and diffusion works in the different models. The concentrations are normalised with the source strength and the undisturbed wind speed at 10 m above ground.

The source in the courtyard (B) is switched on. The emissions are transported to the leeward wall and lift off near the wall. ABC simulates to high concentrations near the plume axes, because the diffusion in the courtyard is too low. ASMUS, which works with the same wind field as ABC, gives better results. DASIM lifts the whole plume above roof level and, cause of very small diffusion coefficients near the ground, the concentrations near the soil are too low, compared with wind tunnel measurements

In Figure 7 the walls of the courtyard are fold up and the concentrations near the walls are displayed. The ABC results show that the transport dominates the diffusion process. ASMUS gives satisfying results in comparison with the wind tunnel concentrations (picture at the bottom), measured at the points indicated by small crosses (be careful while interpreting the contour lines). In MISKAM the diffusion process is too strong.

Figure 8 shows 2 horizontal sections of the flow field for an approach flow of  $120^\circ$ . The biggest differences occur between MISKAM and ABC. MISKAM underestimates the extend of the near wake. This causes big differences for source C (not displayed), but not for sources A and B.

The next 2 figures are showing surface concentrations for source B and the inclined angle ( $120^\circ$ ). Near the ground DASIM and MISKAM are shifting more concentration out of the courtyard than ABC and ASMUS. The first impression is, that there are big differences. But regarding figure 11, which shows plume cross sections at a distance of 40 m and 120 m, one finds, that in all models most of the mass is transported over the roof and therefore the differences are not too strong. ABC and DASIM give the best results.

To study if the numerical models can simulate the interaction of several buildings, a real scenery was taken. Three wind directions, two source positions and one building varying in height are investigated. The figure 12 and 13 are showing first results.

On the next figure (14) some scatter plots with logarithmic axes provide an idea of the errors. The normalised concentrations of wind tunnel and numerical models are plotted against one another. The dotted lines enclose the points which lie within a factor of 10 compared to the wind tunnel, the dashed lines represent a factor of 2.

These are the results for the 28 m high U-shaped building with source at location B. One finds a good agreement for the wind directions  $0^\circ$ ,  $90^\circ$  and  $180^\circ$  for high and middle concentrations. The spread at the other angles is somewhat bigger. At low concentrations the accordance is worse. Practically these concentrations are not of interest, and one can assume errors in measurements grow up at low concentration levels.

The next figure (15) shows some statistics, where all measurements for the 28 m high building system were included. The linear correlation coefficient ranges from 0.4 to somewhat above 0.8. This is a measure for the fit of the higher concentrations. The logarithmic correlation coefficient, which ranges between 0.7 and 0.8, weights all concentration levels in the same manner.

The "hit rate" for factor 2 is about 35%, for a factor of 10 about 75%.

Every model has some defects in wind field, turbulence parameterization and dispersion calculation, which are less or more important at distinct wind directions. Including all directions, one cannot find a "best" model.

The investigation shows, that the model outputs have good qualitative characteristics, but the quantities should be corrected. Nevertheless this study will give the modellers some valuable advice's to improve their models.

## 5. Projects

In the last section two projects should be investigated.

### Wind-discomfort

The first one is a study where high wind speeds near high rised buildings can occur. Near an existing 50 m high building another 71 m high building is planned. Figure 16 shows the flow at a height of 10.5 m above ground. One finds the typical recirculation zones and a speed-up between the buildings. The contour lines of the wind speed normalised with the undisturbed wind speed at same height is displayed on figure 17. The speed-up zones can easily be located. Between the buildings one finds an overspeeding by a factor of 1.5. The physics of the diagnostic flow model lead to an underestimation of this value by a factor of 1.6 to 2. For simple block like structures like in this example, the model is a useful tool to predict speed-up zones.

### Dispersion modelling

In the second example an actual project is invited. Within a settlement the traffic changes in some street systems, cause a new road is planned. For the components benzene,  $\text{NO}_x$  and soot calculations were made for 36 wind directions. From this immission base and the meteorological statistics, representative for one year, mean values and percentiles were estimated.

Figure 18 shows the building arrangement and the line sources, which are taken into account. On the last figure (19) yearly mean concentration levels for benzene are displayed.

A comparison to measuring stations in this area gave satisfying agreement. The concentrations in sheltered areas were much better represented, than with usual Gauß-models.

## References

**Blinda,S., Hopf,A., Manier,G., Marburg,K. 1992**

Entwicklung und Verifizierung eines Rechenmodelles zur Simulation der Ausbreitung von KFZ-Emissionen im Bereich komplexer Gebäudekonfigurationen.

Abschlußbericht für das Ministerium für Umwelt, Raumordnung und Landwirtschaft des Landes Nordrhein-Westfalen. Institut für Meteorologie der Technischen Hochschule Darmstadt.

**Eichhorn,J. 1989**

Entwicklung und Anwendung eines dreidimensionalen mikroskaligen Stadtklima-Modells

Dissertation, Johannes-Gutenberg-Universität Mainz.

**Groß,G. et.al. 1994**

ASMUS – Ein numerisches Modell zur Berechnung der Strömung und der Schadstoffverteilung im Bereich einzelner Gebäude.

To be published in Meteorologische Rundschau.

**Hosker,R.P. 1984**

Flow and diffusion near obstacles. In Atmospheric Science and Power Production, SOE/TIC-27601, ISBN 0-87079-126-5.

**Janicke,L. 1985**

Particle simulation of dust transport and deposition and comparison with conventional models

In Air Pollution Modelling and its Application, IV Plenum Press N Y , 759-769.

**Klein,P., Rau,M., Wang,Z., Plate,E.J. 1994**

Concentrations and flow field in the neighbourhood of buildings and building complexes (wind tunnel experiments). Annual Report, Research Programme for Air Pollution Prevention Measures, Kernforschungszentrum Karlsruhe (in german)

**Röckle,R. 1990**

Bestimmung der Strömungsverhältnisse im Bereich komplexer Bebauungsstrukturen

Dissertation, Technische Hochschule Darmstadt

**Sasaki,Y. 1970**

Some basic formalisms in numerical variational analysis. Mon Weather Rev. 8,44-59.

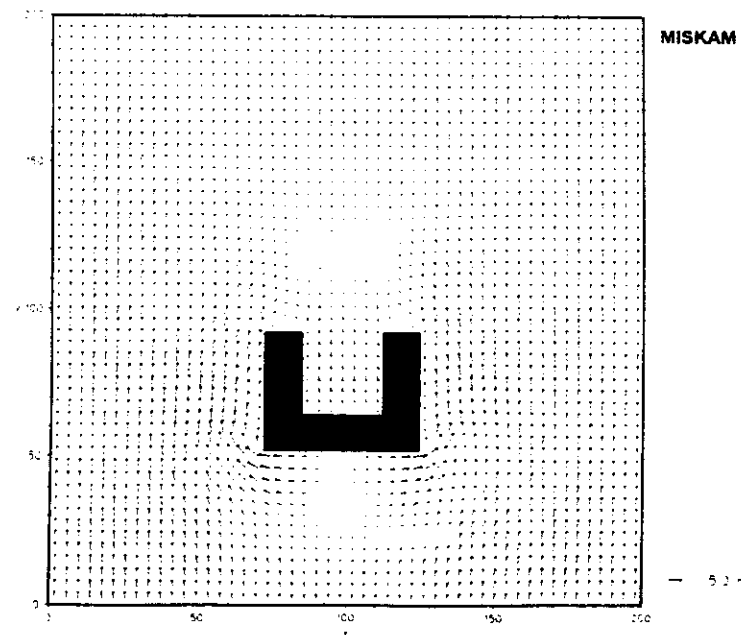
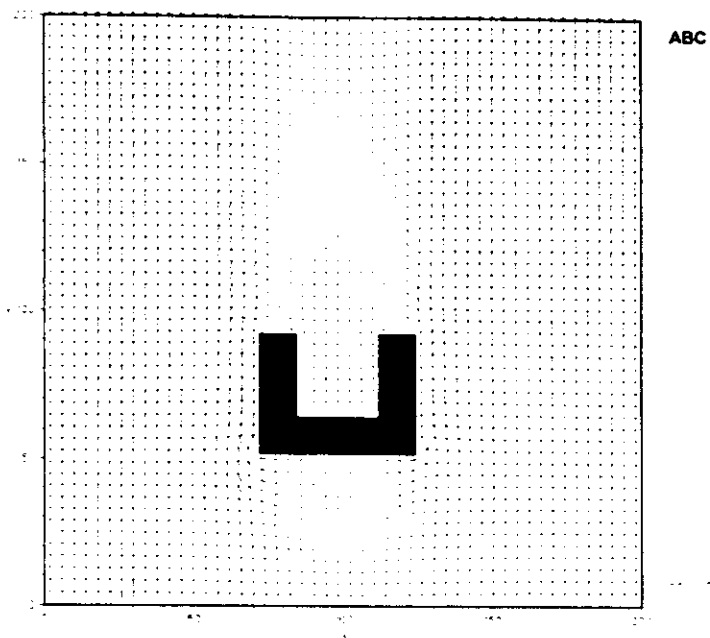
**Sherman,C.A. 1978**

A mass-consistent model for wind fields over complex terrain. J Appl Met. 17, 312-319.

**Shir,C.C., Bornstein,R.D. 1977**

Eddy exchange coefficients in numerical models of the planetary boundary layer. Bound Layer Met. 11, 171-185.

# Flow field near ground



## Vertical section at mid of building approach flow 0°

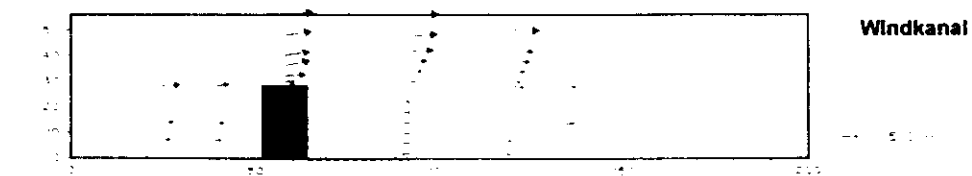
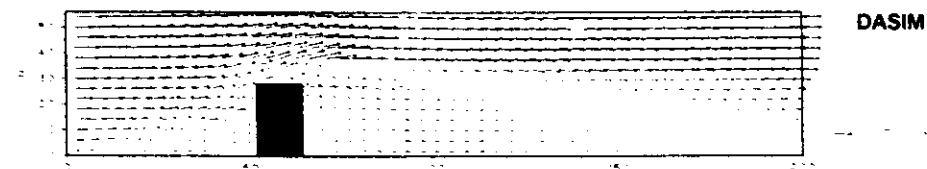
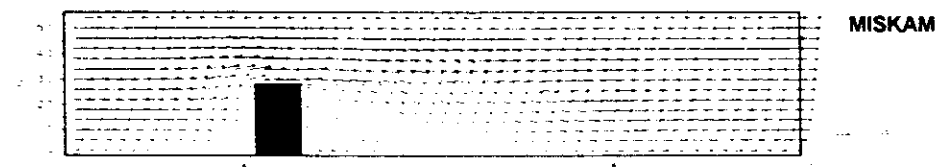
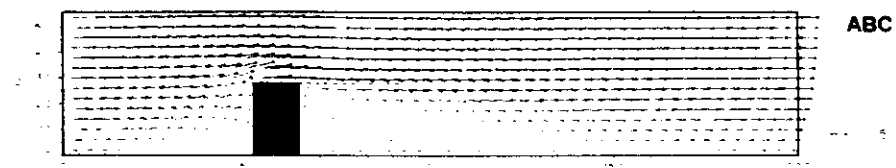


Fig. 4



**Concentrations**  
Vertical section at mid of building

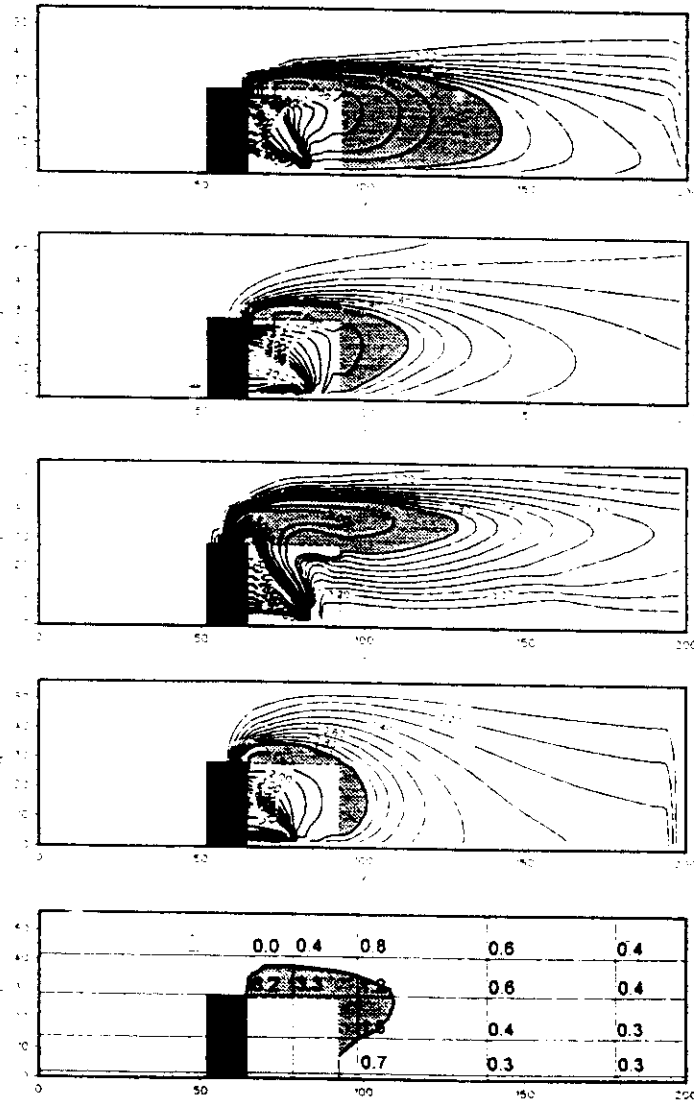


Fig. 6

**Diffusion coefficients**  
Vertical section at mid of building

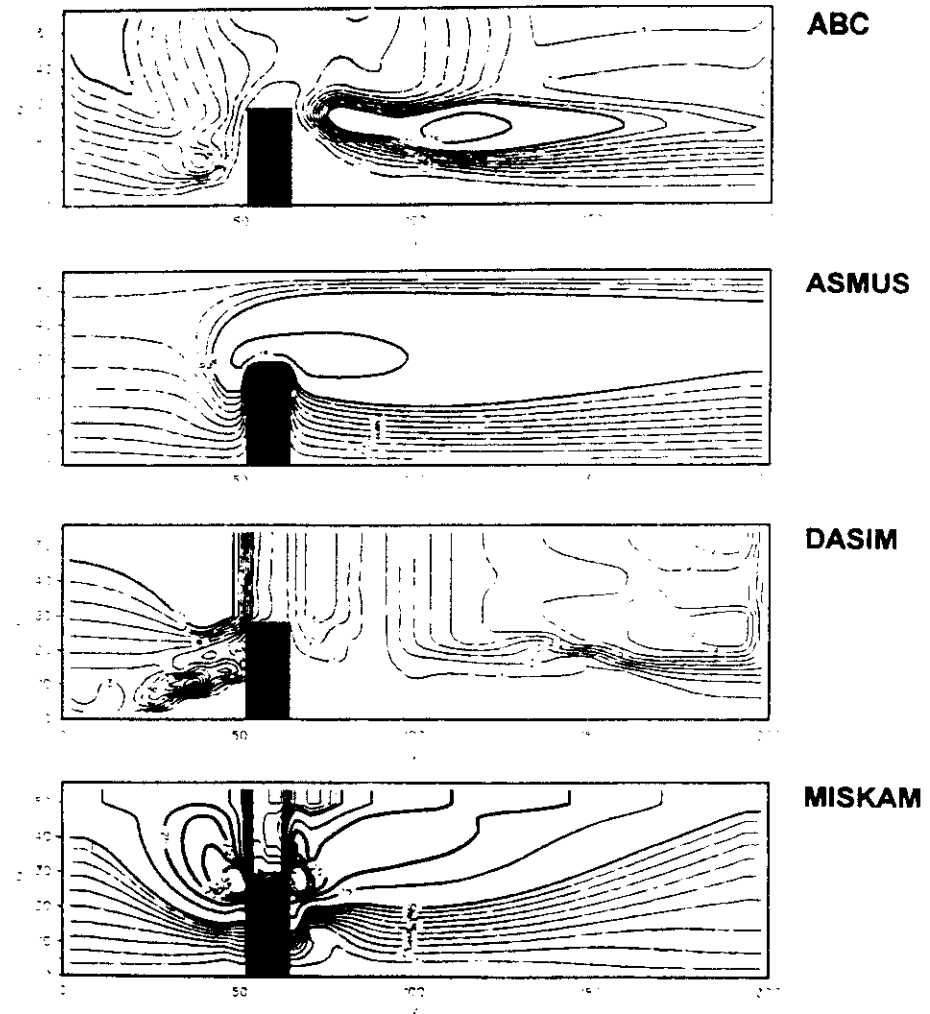
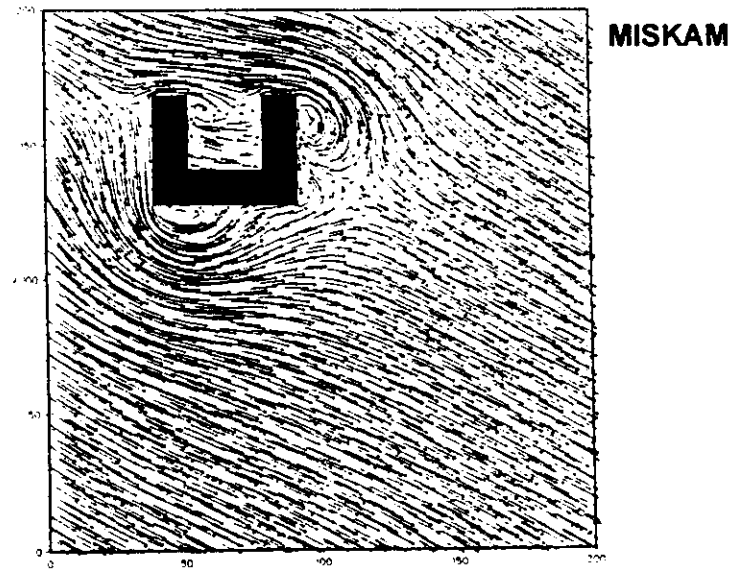
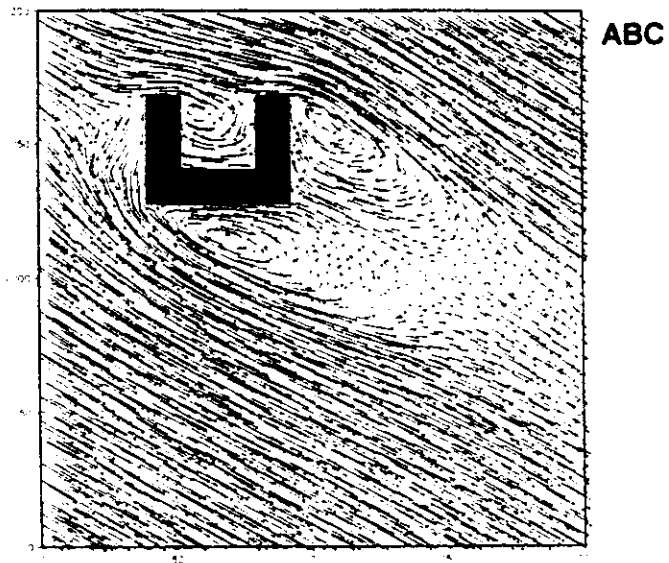
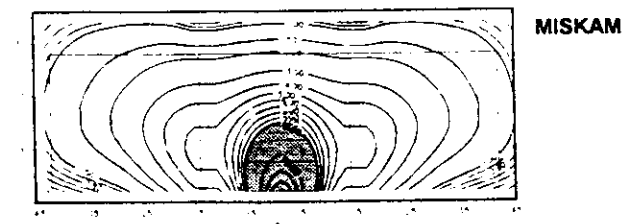
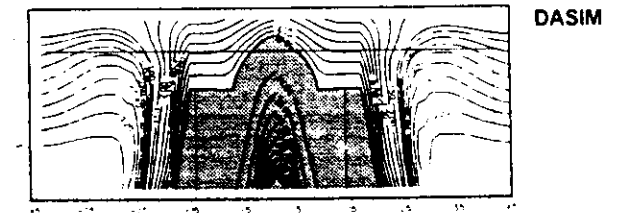
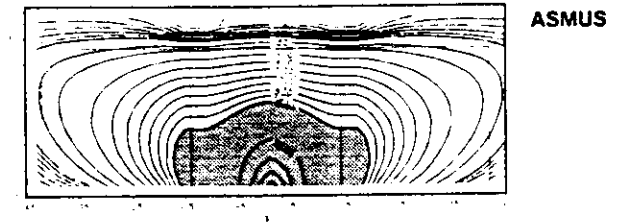
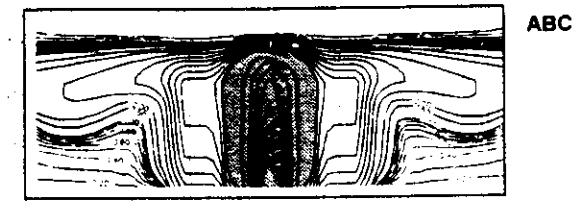


Fig. 5

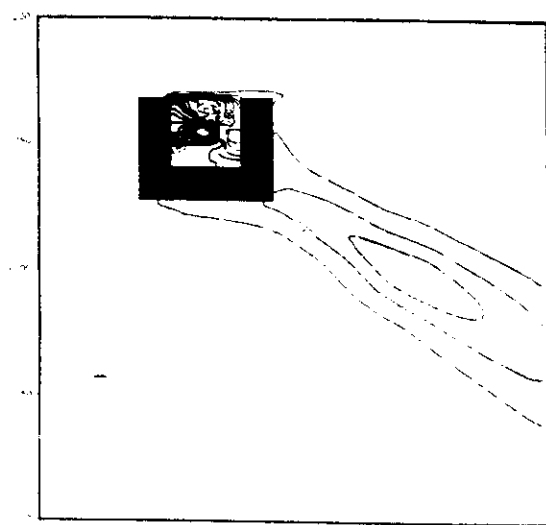
**Flow field near ground  
Approach flow 120°**



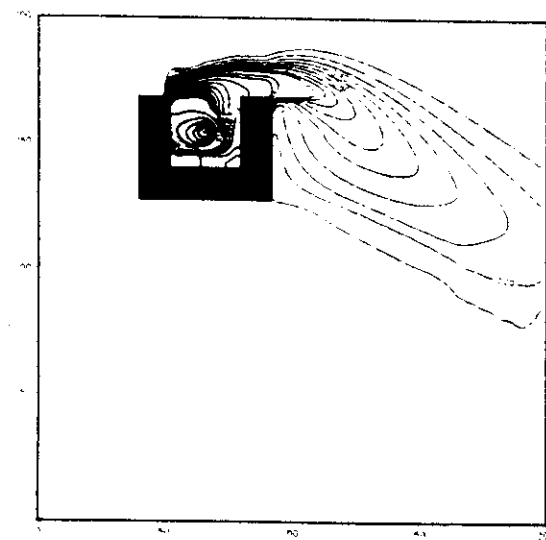
**Concentration near walls of courtyard**



Surface concentration, Source B  
Approach flow 120°



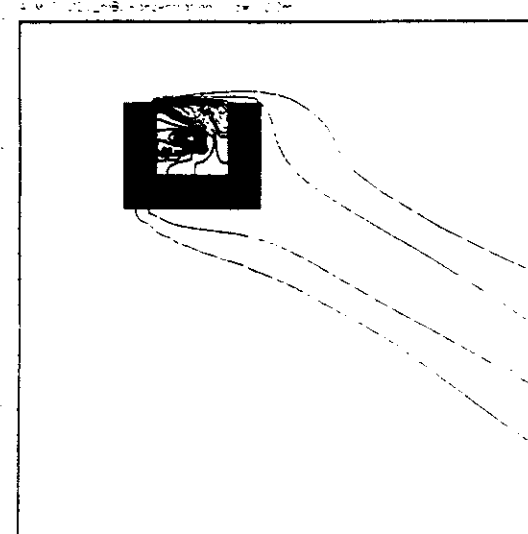
ABC



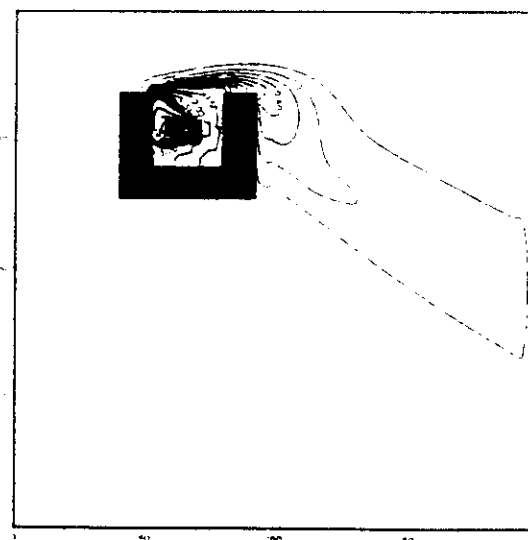
DASIM

Fig 9

Surface concentration, Source B  
Approach flow 120°



ASMUS



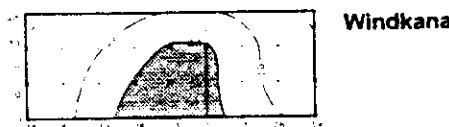
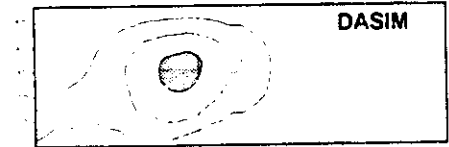
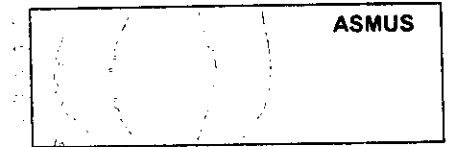
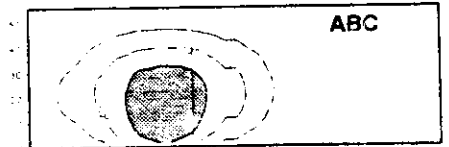
MISKAM

Fig. 10

**Plume cross sections  
Source B, Approach flow 120°**

Distance 40 m

Distance 120 m



Windkanal

**Trajectories**  
**Source on top of roof and near the bottom**  
**of the street canyon**

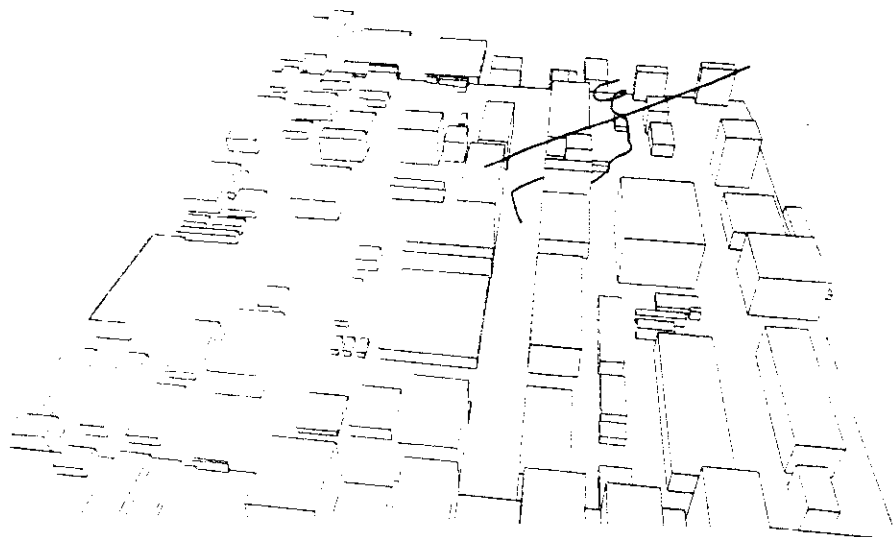


Fig. 12

**typical flow field**

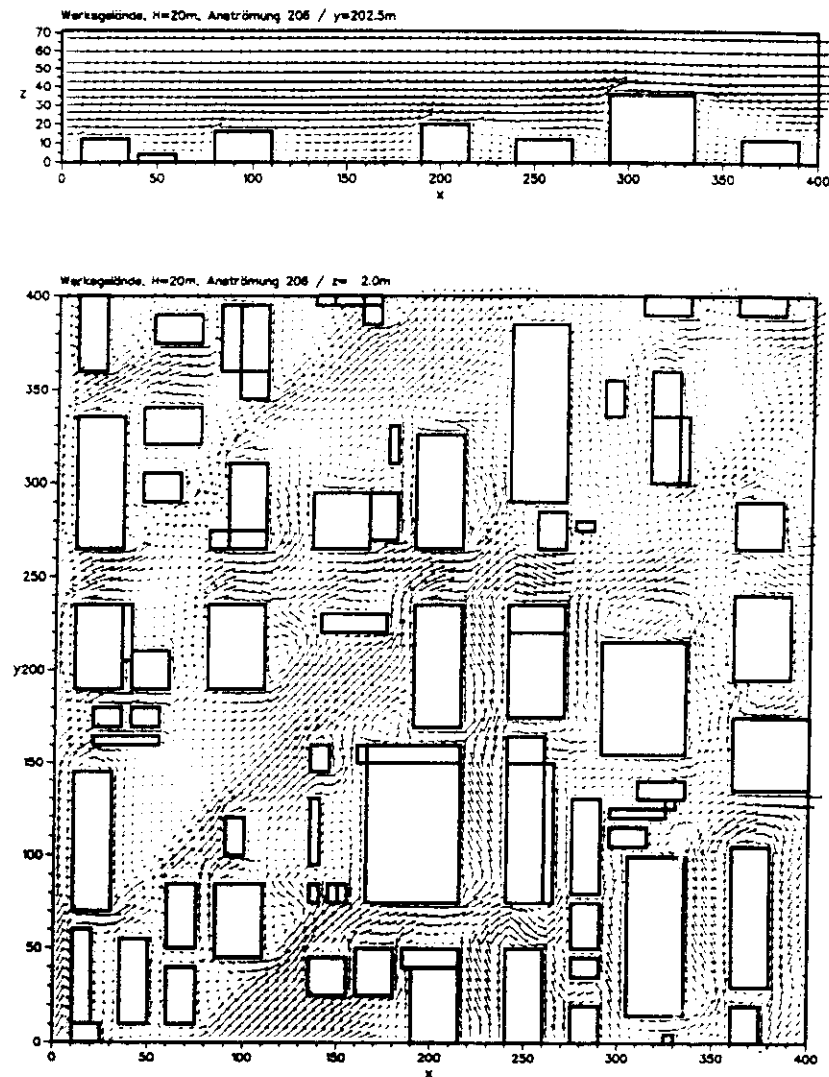
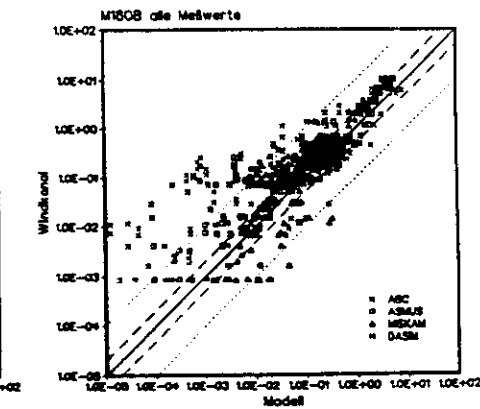
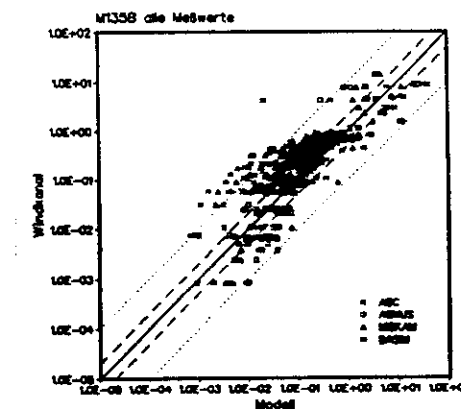
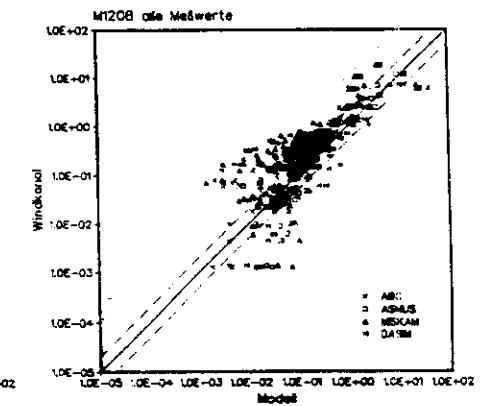
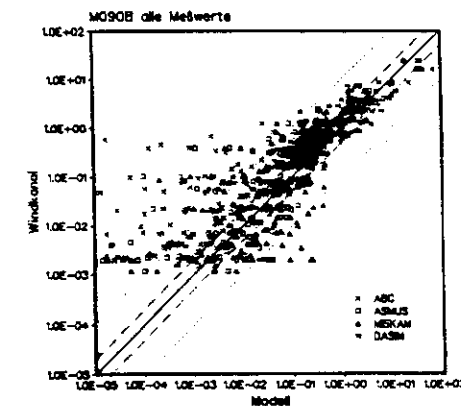
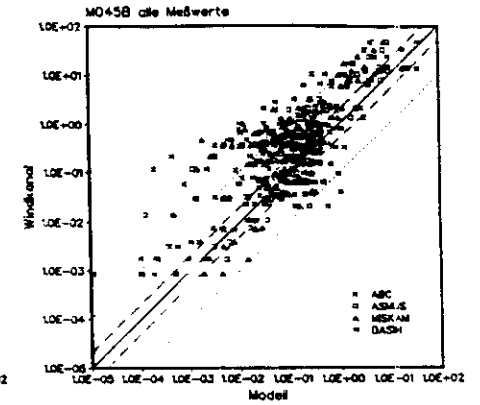
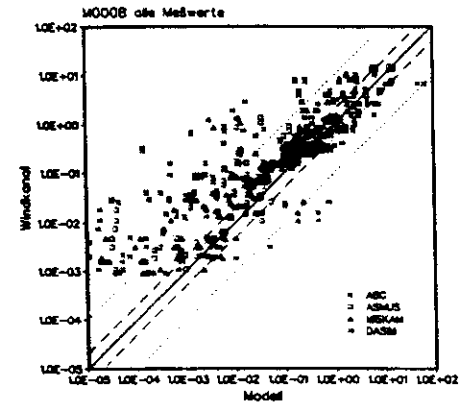
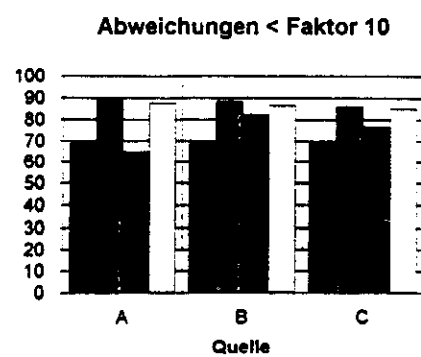
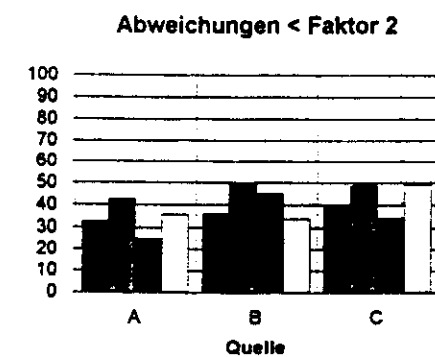
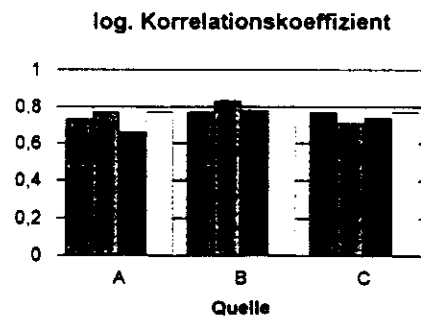
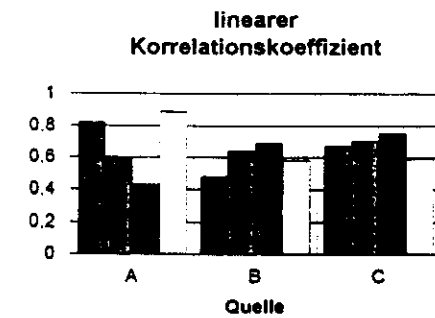
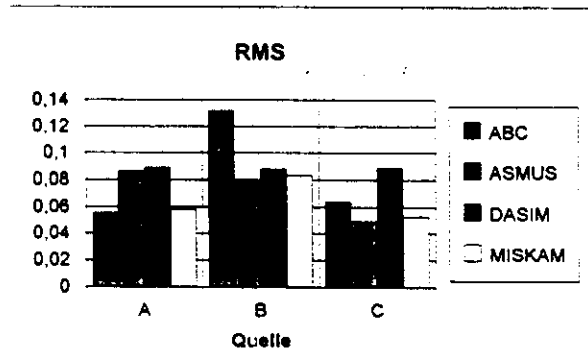


Fig. 13

# Statistik



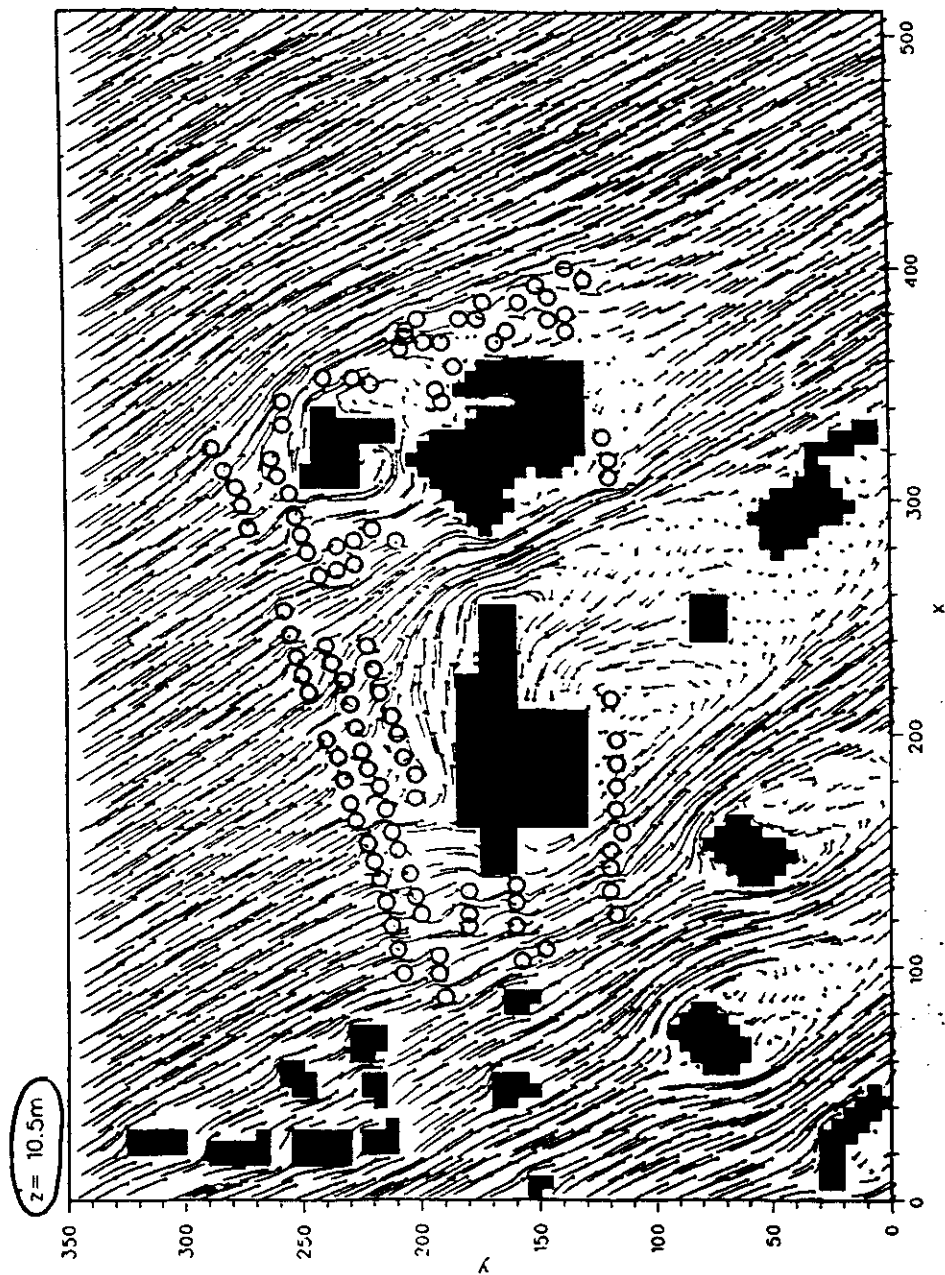


Fig. 16

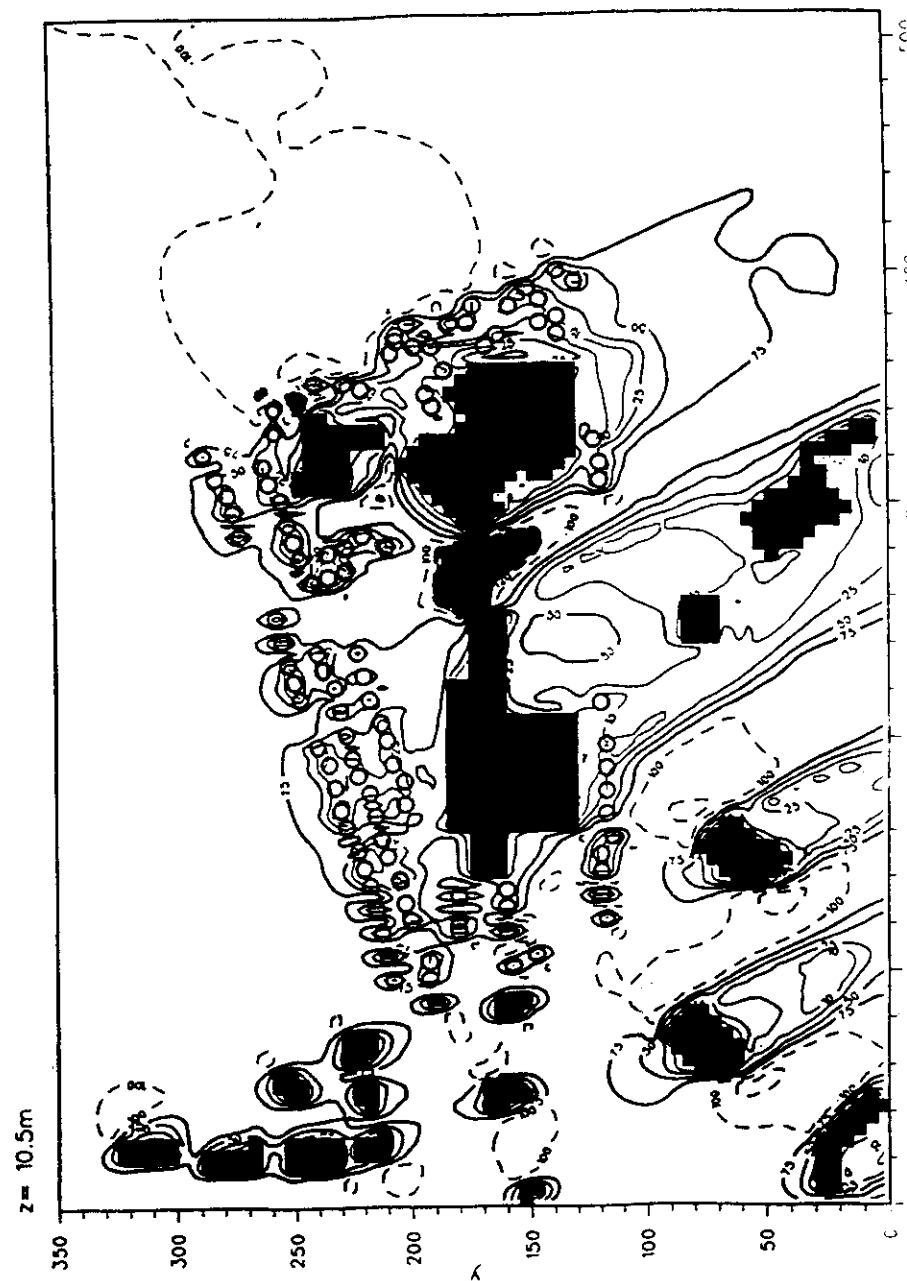


Fig. 17

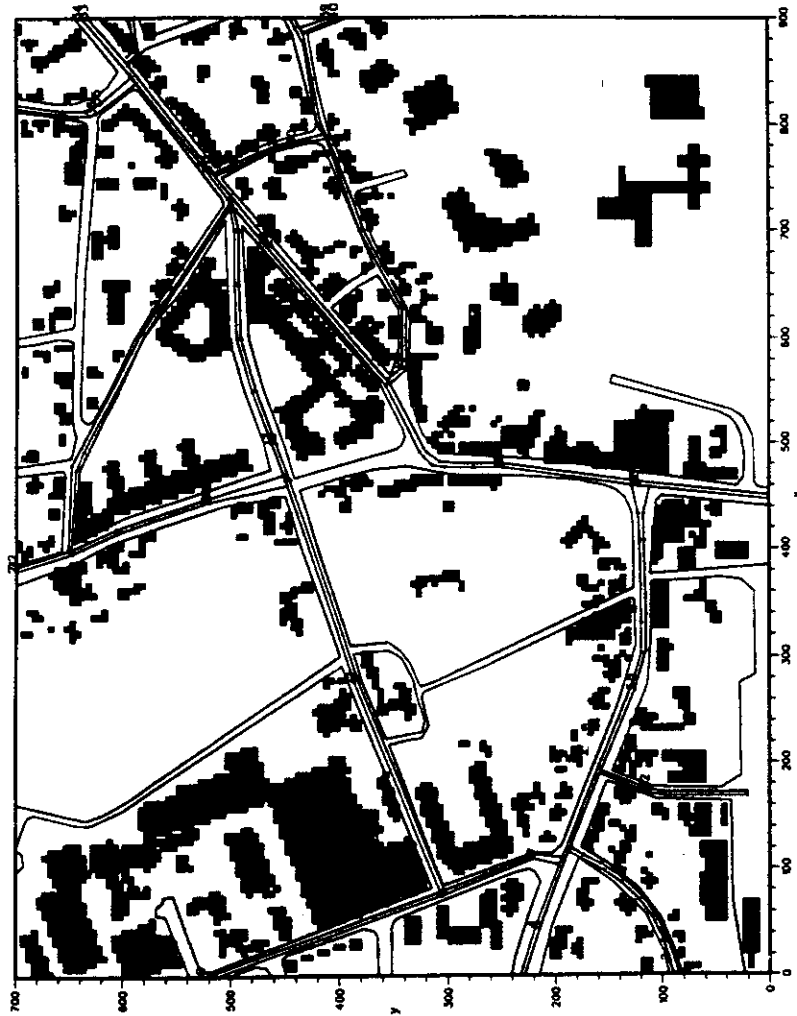


Fig. 18

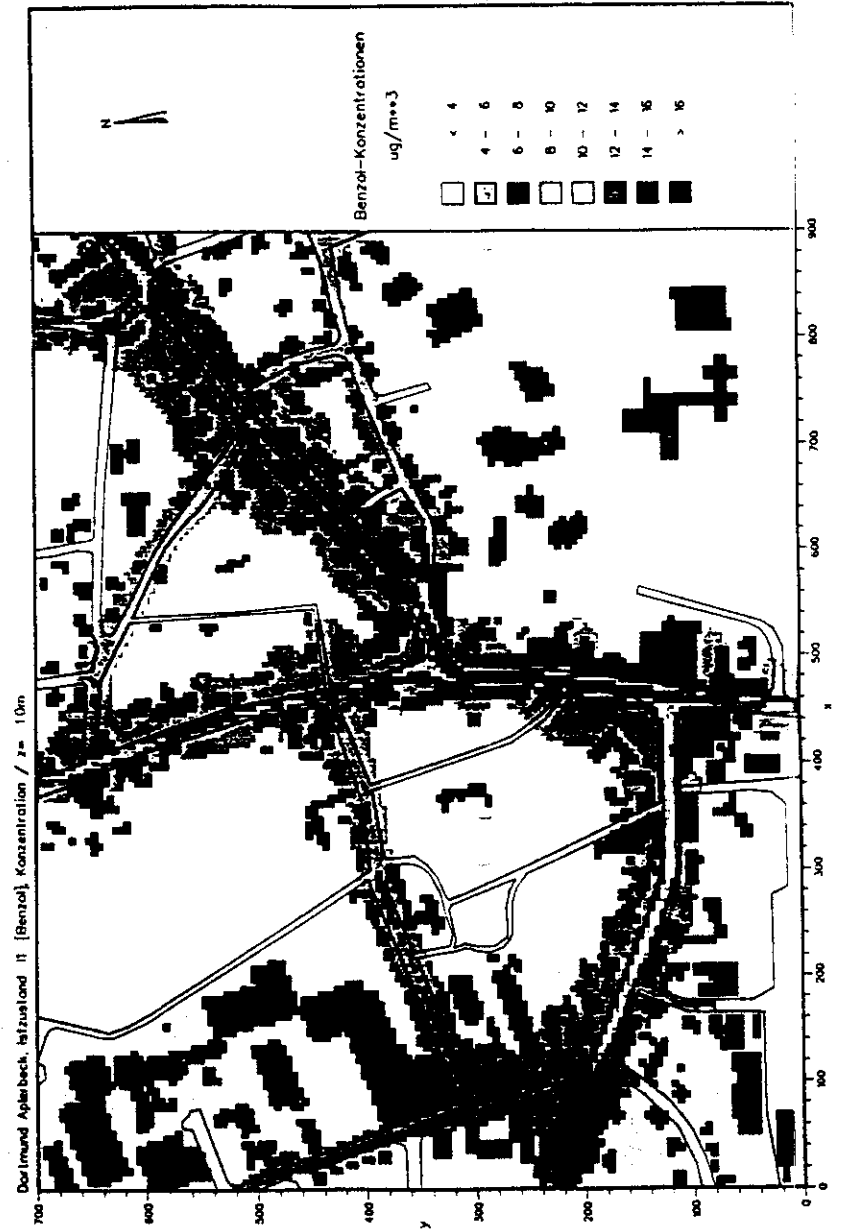


Fig. 19